Annals of Warsaw University of Life Sciences – SGGW
Agriculture No 69 (Agricultural and Forest Engineering) 2017: 89–97
(Ann. Warsaw Univ. of Life Sci. – SGGW, Agricult. 69, 2017)
DOI 10.22630/AAFE.2017.10

Simulation model of three phase induction motor

RAFAŁ KORUPCZYŃSKI
Department of Fundamental Engineering, Warsaw University of Life Sciences – SGGW

Abstract: *Simulation model of three phase induction motor*. In this paper a simulation model of induction motor has been proposed. The model has been realized in the Spice-class software. The complete system of differential equations describing of induction motor has been presented. Results has shown, that there is possibility of electric drive system simulation in electronic simulation software. Step response curves of motor parameter for a change of load torque has been presented.

Key words: induction motor, simulation, LTSpice, dynamic system

INTRODUCTION

Electric motors are widely used in an economy. It has been estimated, that about 40 to 45% of overall electrical energy has been consumed by motors [Waide et al. 2011, Van Werkhoven et al. 2016]. The induction motors are most often used type of motors. The advantages are reliable structure, low material and manufacturing cost [Hu et al. 2016]. In agriculture, electric motors drive farm machines such as: chaff-cutters, threshes or milking machines [Goźlińska 2015] and pumps, conveyors [Waide et al. 2011]. From the research and design point of view, the key problem is a mutual cooperation of all system parts. This issue may be tested by computer simulation. Apart the mechanical system there is a demand of simulation of electric drive, including induction motor.

There are some numerous publications about induction motor simulation. Unfortunately, most of them require Matlab/Simulink software for calculations [Okoro 2003, Soe et al. 2008, Aktaibi et al. 2011, Gupta et al. 2014, Jain et al. 2014, Phukon et al. 2015]. This software package has only one drawback – high price. This research is based on the LTSpice software, which is free. In this paper, the three phase, symmetric, squirrel-cage induction motor is considered only. Because of simpler and cheaper rotor construction, this type of motor is widespread used.

MATHEMATICAL MODEL OF THREE PHASE INDUCTION MOTOR

From the circuit theory, supply stator voltages of any phase (*a*, *b* and *c*) are equal [Latek 1982, Popescu 2000, Gao et al. 2004]:

$$u_{as} = R_{sa} i_{as} + \frac{d\Psi_{as}}{dt} \qquad (1)$$

$$u_{bs} = R_{bs} i_{bs} + \frac{d\Psi_{bs}}{dt} \tag{2}$$

$$u_{cs} = R_{cs} i_{cs} + \frac{d\Psi_{cs}}{dt} \tag{3}$$

Rotor voltages are equal:

$$u_{ar} = R_{ar} i_{ar} + \frac{d\Psi_{ar}}{dt} \tag{4}$$

$$u_{br} = R_{br} i_{br} + \frac{d\Psi_{br}}{dt} \tag{5}$$

$$u_{cr} = R_{cr} i_{cr} + \frac{d\Psi_{cr}}{dt} \tag{6}$$

where: $u_{\dots s}$ $u_{\dots r}$ are stator or rotor voltages [V] respectively (in the case of squirrel-cage motor $u_{\dots r} = 0$); $R_{\dots s}$, $R_{\dots r}$ are stator and rotor resistances [Ω]; $i_{\dots s}$, $i_{\dots r}$ are stator and rotor currents [A]; $\Psi_{\dots s}$, $\Psi_{\dots r}$ are flux linkages [Wb] of stator and rotor.

The flux linkages are functions of self and mutual inductances. The last ones are complicated functions of rotor position and current on the machine windings [Gao et al. 2004]. Because of this complexity, some other authors proposed model, based on two orthogonal windings: one pair for the stator and second for the rotor [Otýpka 2016]. Hence, three phase machine changes to equivalent two phase machine. The translation requires of application so-called space vector theory [Żelechowski 2005]. The advantage of this procedure is the transformation of stator and rotor voltages, currents and fluxes to common frame of reference (coordinate system) [Krause et al. 1965]. This system may be rotating with arbitrary angular speed ω or rotor angular speed ω_m, or to stationary coordinate system fixed with rotor (not rotating, $\omega = 0$). The last case is realized in this paper.

Hence, inductances are not joint to rotor position [Simion et al. 2012]. The voltage equations from [Żelechowski 2005] are transformed with conversion of rotor quantities on stator side (finally marked by r and ′) as it has shown in [Latek 1982]:

$$u_{s\alpha} = R_s i_{s\alpha} + \frac{d\Psi_{s\alpha}}{dt} \tag{7}$$

$$u'_{r\alpha} = 0 = R_r i'_{r\alpha} + \frac{d\Psi'_{r\alpha}}{dt} + p_b \omega_m \Psi'_{r\beta} \tag{8}$$

$$u_{s\beta} = R_s i_{s\beta} + \frac{d\Psi_{s\beta}}{dt} \tag{9}$$

$$u'_{r\beta} = 0 = R'_r i'_{r\beta} + \frac{d\Psi'_{r\beta}}{dt} - p_b \omega_m \Psi'_{r\alpha} \tag{10}$$

The flux linkages equations are [Krause et al. 2002]:

$$\Psi_{s\alpha} = (L_{ls} + L_M) i_{s\alpha} + L_M i'_{r\alpha} \tag{11}$$

$$\Psi'_{r\alpha} = (L'_{lr} + L_M) i'_{r\alpha} + L_M i_{s\alpha} \tag{12}$$

$$\Psi_{s\beta} = (L_{ls} + L_M) i_{s\beta} + L_M i'_{r\beta} \tag{13}$$

$$\Psi'_{r\beta} = (L'_{lr} + L_M) i'_{r\beta} + L_M i_{s\beta} \tag{14}$$

where: α and β denotes first and second component of stationary coordinate system. They match positive parts of x and y axis of Cartesian coordinate system respectively; L_{ls}, L_{lr}' [H] are the stator or rotor windings leakage inductances; L_M [H] is magnetizing inductance and p_b is number of pole pairs, which is a constructional parameter of given motor. Resistances and inductances in above equations can be calculated based on free-running and locked rotor motor tests, and resistance measurements [Latek 1982].

Three phase induction motor torque, called electromagnetic torque T_e [Nm] can be written as [Salahat 2011]:

$$T_e = \frac{3}{2} p_b (\Psi_{s\alpha} i_{s\beta} - \Psi_{s\beta} i_{s\alpha}) \tag{15}$$

Because of rotating nature of drive system with electric motor, equation of motion, based on Newton' second law, is described by [Okoro 2004]:

$$T_e - T_l = J \frac{d\omega_m}{dt} \tag{16}$$

where: T_l is the load torque [Nm], J is the total moment of inertia of drive system [kg·m^{-2}], ω_m is rotor angular speed [rad·s^{-1}].

Input quantities of induction motor model are three phase supply voltages and load torque, output – three phase stator currents, electromagnetic torque and rotor angular speed. Equations 7–14 need of calculations α, β (two phase) components from three phase (a, b, c) quantities and vice versa.

Clarke transformation allows to convert any quantity f_{abc} to quantity $f_{\alpha\beta}$ by formula [Chattopadhyay et al. 2011, Microsemi 2013]:

$$f_\alpha = f_a \tag{17}$$

$$f_\beta = \frac{1}{\sqrt{3}}(f_a + 2f_b) \tag{18}$$

Inverse Clarke transformation is as follows:

$$f_a = f_\alpha \tag{19}$$

$$f_b = \frac{1}{2}(-f_\alpha + \sqrt{3} f_\beta) \tag{20}$$

$$f_c = \frac{1}{2}\left(-f_\alpha - \sqrt{3} f_\beta\right) \tag{21}$$

Mathematical equations 7–21 are basis of motor simulation model construction in LTSpice software.

SIMULATION MODEL OF THREE PHASE INDUCTION MOTOR

The first part of simulation model is presented on Figure 1. Voltage sources V4–V6 are three-phase power supply: 3 × 400 V, 50 Hz. Current sources BI1-3 are implementation of inverse Clarke transform of currents $i_{\alpha\beta}$ to i_{abc} (eqn. 19––21). Labels A–C allows for convenient voltage measurement. Resistor R6 is only for numerical reason – each part of circuit have to have one grounded node. On the Figure 2 is the second part of model. Sources: BV_salfa, BV_sbeta are implementation of Clarke transform: u_{abc} to $u_{\alpha\beta}$ (eqn. 17–18). Zero-voltage sources: V_ralfa, V_rbeta are left side of equations 8 and 10. B1 and B2 sources are last part ($\pm p_b$ …) of equations 8 and 10 respectively. Voltage sources: BPsi… (Fig. 3) calculate flux linkages from equations 11–14. Schematic diagram of

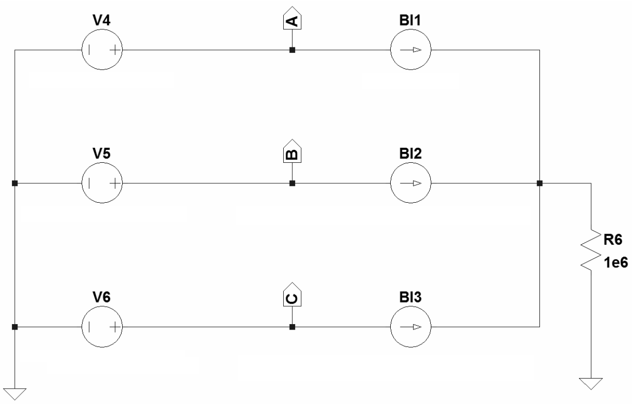

FIGURE 1. Electrical circuit of simulation model – part 1

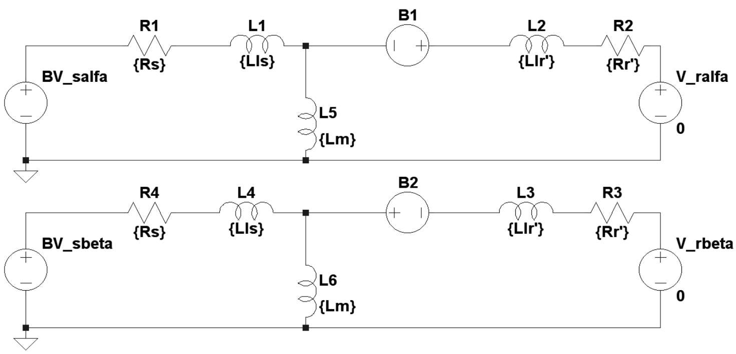

FIGURE 2. Electrical circuit of simulation model – part 2

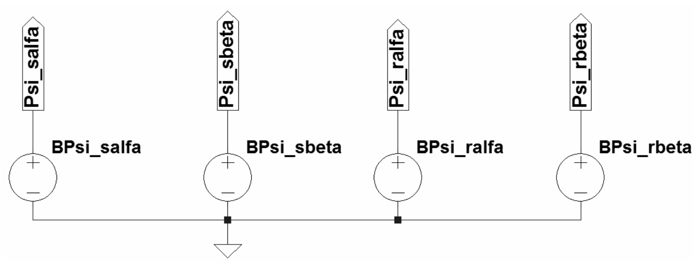

FIGURE 3. Electrical circuit of simulation model – part 3

circuit, which is realization of mechanical part of simulation model is shown on Figure 4.

Electromagnetic torque is calculated (eqn. 15) by voltage source BV_Me, whereas load torque is set by voltage source V_TL (both cases 1 V for 1 Nm). Rotor angular speed ω_m as a current of inductor L7 is integrated in circuit on Figure 4. Resistor R5 is from point of view of numerical stability. The approach of dynamical simulation of mechanical sys-

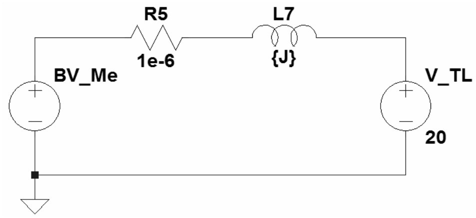

FIGURE 4. Electrical circuit of simulation model – part 4

tems in electric simulation software have been presented in [Korupczyński 2016]. Parameters of modeled three phase squirrel-cage induction motor are shown on Table. They are based on the literature [Simion et al. 2012]. Rotational speed n [min^{-1}] (the Table) can be calculated from angular speed by the formula:

$$n = \frac{30}{\pi} \cdot \omega \tag{22}$$

TABLE. Parameters of simulated motor

Parameter	Value
P_n [kW]	4.0
U_n [V]	400
I_n [V]	8.1
n_n [min^{-1}]	1,440
T_n [Nm]	26.5
R_s [Ω]	1.1
R_r'[Ω]	0.95
L_{ls} [mH]	9.5
L_{lr}'[mH]	9.5
L_m [mH]	172.7
p_b [-]	2
J [kg·m^{-2}]	0.02

RESULTS AND DISCUSSION

The first simulation concerns of motor startup and idle state for nominal supply conditions. For convenience, rotor angular speed ω_m have substituted by rotational speed n. Torque T_e, phase current I and speed n waveforms are presented on Figures 5 and 6. All waveforms in this paper have been prepared in Octave software (www.octave.org).

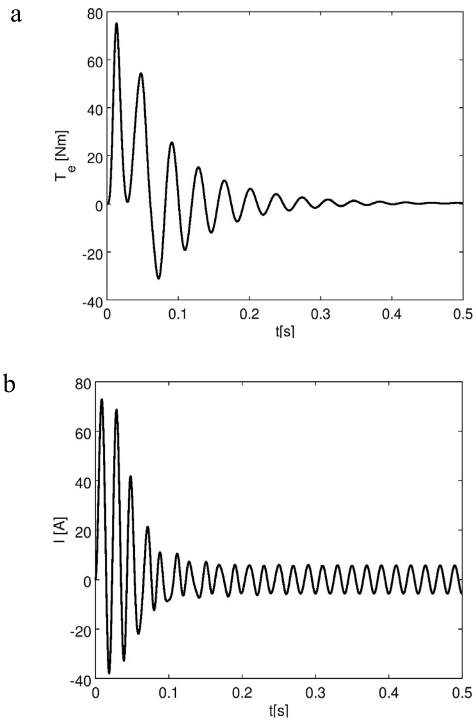

FIGURE 5. Electromagnetic torque T_e (a) and phase current I (b) versus time t (idle state)

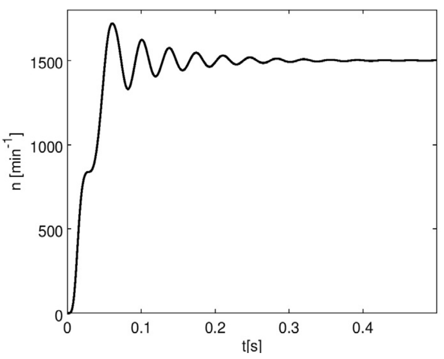

FIGURE 6. Rotational speed n versus time t (idle state)

For the first moment of time, the torque, current and rotational acceleration (d*n*/d*t*) have high values (Figs 5–6). When the speed is going up, the torque and current are going down. There are some oscillations of rotational speed (Fig. 6). The startup time is less than 0.1 s. Steady state current is about 4.2 A (Root Mean Square – *RMS*), steady state speed is 1,499 min^{-1}. It should be noted, that in the real conditions at the starting moment the supply voltage is slightly going down, because of high current is flowing. In all simulations supply voltage has constant value the whole time.

The second simulation have been performed for startup and load with constant T_l = 21 Nm. Waveforms are shown on Figures 7 and 8. Startup time is slightly more than 0.2 s and steady-state speed is 1,465 min^{-1} (Fig. 8). During the startup time, phase current *I* is more than 28.4 A (RMS). At steady-state current is going down to 6.8 A (Fig. 7). From time value of 0.2 s electromagnetic torque T_e oscillates around value 21 Nm, which is equal of load torque T_l. In this case mechanical power P_m as as product o load torque and angular speed in steady-state is about 3,200 W.

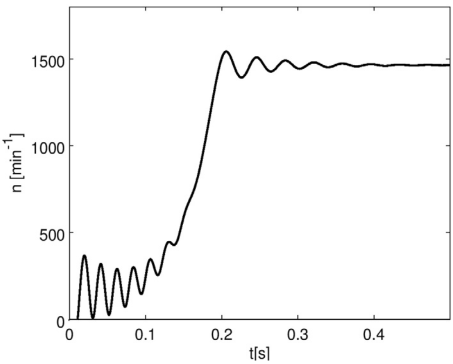

FIGURE 8. Rotational speed *n* versus time *t* (T_l = = 21 Nm)

The other simulations concern of step change of load torque T_l and return to idle state after idle startup. Two cases are considered: value of load torque change ΔT_l is equal 26.5 Nm or 53 Nm. Waveforms are presented on Figures 9–12. Dynamic changes of parameters can be analyzed quite easily. The startup process is the same on both cases. The higher load torque T_l cause build-up of phase current: 8.1 A and 16.3 A (*RMS*) respectively

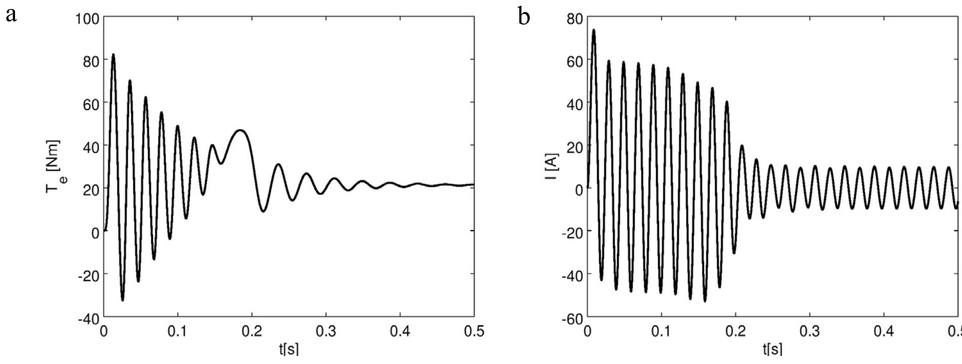

FIGURE 7. Electromagnetic torque T_e (a) and phase current *I* (b) versus time *t* (T_l = 21 Nm)

a b
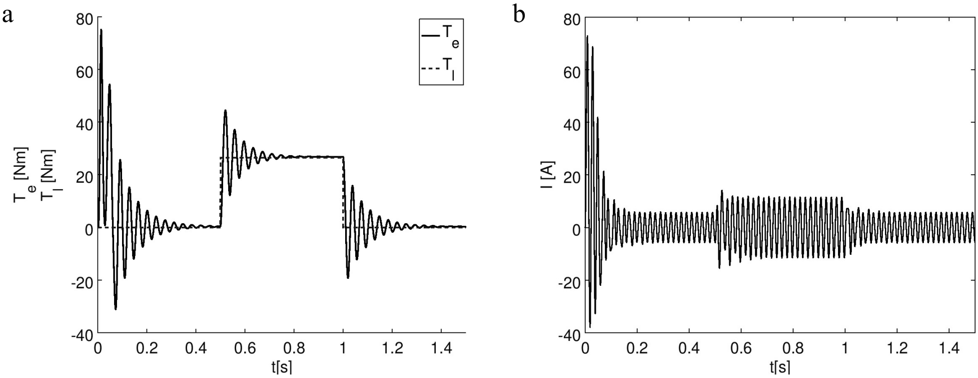

FIGURE 9. Electromagnetic torque T_e (a) and phase current I (b) versus time t (step change $\Delta T_l = 26.5$ Nm)

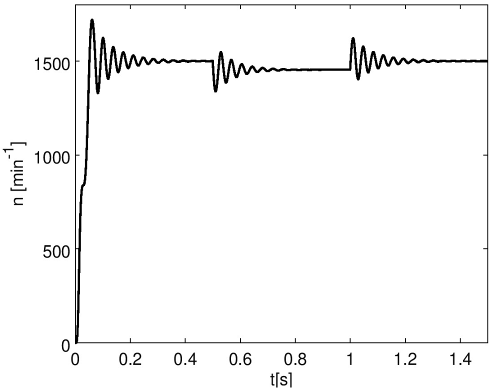

FIGURE 10. Rotational speed n versus time t (step change $\Delta T_l = 26.5$ Nm)

a b
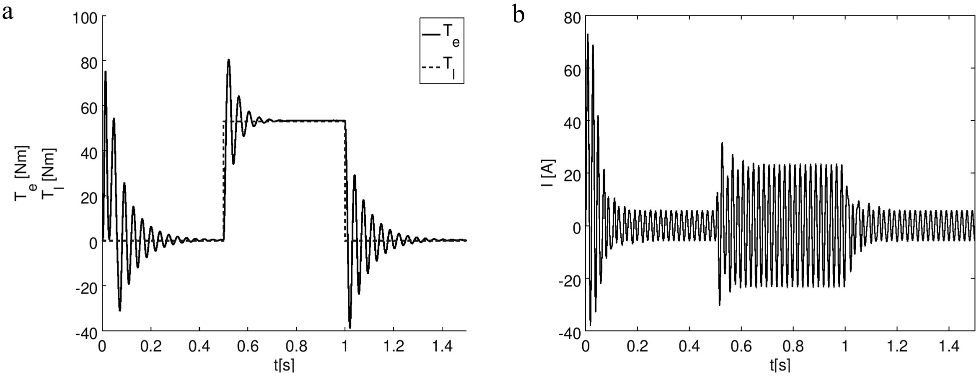

FIGURE 11. Electromagnetic torque T_e (a) and phase current I (b) versus time t (step change $\Delta T_l = 53$ Nm)

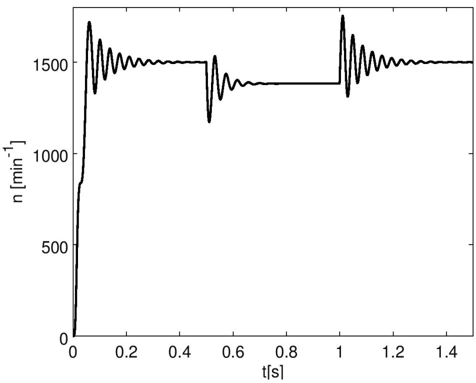

FIGURE 12. Rotational speed *n* versus time *t* (step change $\Delta T_l = 53$ Nm)

(cf. middle part current waveform of Figs 9 and 11). Simultaneously, the speed is significantly going down: 1,460 min^{-1} and 1,386 min^{-1} respectively (cf. middle part of Figs 10 and 12).

It should be noted that steady-state mechanical power P_m (calculated as product o load torque and angular speed after loading of motor) is going up from 3,980 W ($T_l = T_e = 26.5$ Nm) to 7,690 W ($T_l = T_e = 53$ Nm). The second value can indicate motor overheating. Computer simulation has strong advantage: there is no risk of motor damage. In the steady-state always load torque is equal electromagnetic torque: $T_l = T_e$ (cf. torque waveform of Figs 9 and 11). Moreover, step change of load triggers oscillations of T_e and *n* waveform. From the control theory point of view, motor has to be considered as oscillating system. As is shown above, the first value of step change of load torque is equal of nominal motor torque T_n (the table). In this case, calculated mechanical power P_m is very close to nominal motor power P_n (the table). Hence, accuracy of simulations can be recognize as sufficient.

SUMMARY

In the paper, the complete simulation model of induction motor have been presented. It can be used in wide accessible software. The model allows to analyze dynamical states in drive systems, also at the design stage. Motor and working machinery data and characteristics are required. From the result of simulations of particular motor it is clear, that some parameters of system can be determined quite easily and quickly. Moreover, there is no risk of equipment failure, e.g. due accidental excess of nominal parameters.

REFERENCES

AKTAIBI A., RAHMAN M.A. 2011: Dynamic Simulation of a Three-Phase Induction Motor Using Matlab Simulink, the 20th Annual Newfoundland Electrical and Computer Eng. Conference (NECEC 2011).

CHATTOPADHYAY S. MITRA M., SENGUPTA S. 2011: Electric Power Quality, Power Systems. Springer Science+Business Media B.V.

GAO W., SOLODOVNIK E.V., DOUGAL R. A. 2004: Symbolically aided model development for an induction machine in virtual test bed. IEEE Transactions on Energy Conversion 19 (1): 125–135.

GOŹLIŃSKA E. 2015: Maszyny elektryczne. Wydawnictwa Szkolne i Pedagogiczne, Warszawa

GUPTA S., WADHWANI S. 2014: Dynamic Modeling of Induction Motor Using Rotor Rotating Reference Frame. International Journal of Innovative Research in Science, Engineering and Technology 3 (6): 10132–10140.

HU Z., HAMEYER K. 2016: A Method of Constraint Handling for Speed-Controlled Induction Machines. IEEE Transactions on Industrial Electronics 63 (7): 4061–4072.

JAIN S.K., SHARMA F., BALIWAL M.K. 2014: Modeling and Simulation of an Induction Motor. International Journal of Engineering Research and Development 10 (4): 57–61.

KORUPCZYŃSKI R. 2016: Simulation model of wind turbine mechanical part. Annals of Warsaw University of Life Sciences – SGGW, Agriculture (Agricultural and Forest Engineering) 68: 95–102.

KRAUSE P.C., THOMAS C.H. 1965: Simulation of symmetrical induction machinery. IEEE Transactions on Power Apparatus and Systems 84 (11): 1038–1053.

LATEK W. 1982: Teoria maszyn elektrycznych. WNT, Warszawa.

Microsemi 2013: Park, Inverse Park and Clarke, Inverse Clarke Transformations MSS Software Implementations User Guide, Microsemi Corporation.

OKORO O.I. 2003: MATLAB simulation of induction machine with saturable leakage and magnetizing inductances. The Pacific Journal of Science and Technology 5 (1): 5–15.

OTÝPKA J., ORSÁG P., STÝSKALA V., KOLOSOV D., KOCMAN S., VAINSTEIN F. 2016: The Enlarged dq Model of Induction Motor with the Iron Loss and Saturation Effect of Magnetizing and Leakage Inductance. In Intelligent Systems for Computer Modelling. Springer International Publishing: 11–22.

PHUKON L.J., BARUAH N. 2015: A Generalized Matlab Simulink Model of a Three Phase Induction Motor. International Journal of Innovative Research in Science, Engineering and Technology 4 (5): 2926–2934.

POPESCU M. 2000: Induction Motor Modelling for Vector Control Purposes, Helsinki University of Technology, Laboratory of Electromechanics, Report. Espoo.

SALAHAT M., BARBARAWE O., ZALATA M. A., ASAD S. 2011: Modular Approach for Investigation of the Dynamic Behavior of Three-Phase Induction Machine at Load Variation. Engineering 3 (05): 525–531.

SIMION A., LIVADARU L., MUNTEANU A. 2012: Mathematical Model of the Three-Phase Induction Machine for the Study of Steady-State and Transient Duty Under Balanced and Unbalanced States. In: Induction Motors-Modelling and Control. InTech: 3–43.

SOE N.N., YEE T.T.H., AUNG S.S. 2008: Dynamic modeling and simulation of three-phase small power induction motor. World academy of science. Engineering and Technology 42 (79): 421–424.

Van WERKHOVEN M., WERLE R. 2014: Cross-cutting measures – leveraging policies and programs. Electric Motor Systems, Workshop – Accelerating energy efficiency in industrial SMEs, IEA Paris 27 November 2014.

WAIDE P., BRUNNER C.U. 2011: Energy-Efficiency Policy Opportunities for Electric Motor-Driven Systems. Working Paper, International Energy Agency.

ŻELECHOWSKI M. 2005: Space vector modulated direct-torque controlled (dtc-svm) inwerter-fed induction motor drive. PhD thesis, Warszawa [manuscript].

Streszczenie: *Model symulacyjny trójfazowego silnika indukcyjnego*. W artykule opisano model symulacyjny trójfazowego silnika indukcyjnego, klatkowego. Model został zrealizowany w oprogramowaniu LTSpice, przeznaczonym do symulacji obwodów elektronicznych. Na podstawie literatury przyjęto układ równań różniczkowych i algebraicznych, który został przekształcony na równoważny mu obwód elektryczny. Uzyskane rezultaty potwierdziły przydatność metody symulacyjnej do analizy stanów dynamicznych układów napędowych z silnikami indukcyjnymi. Zaprezentowano odpowiedzi parametrów silnika na skokowe zmiany napięcia zasilającego i momentu obciążenia.

MS received June 2016

Author's address:
Rafał Korupczyński
Wydział Inżynierii Produkcji SGGW
Katedra Podstaw Inżynierii
02-787 Warszawa, ul. Nowoursynowska 164
Poland
e-mail: rafal_korupczynski@sggw.pl